A&A manuscript no.
(will be inserted by hand later)

Your thesaurus codes are:
08.03.1 - 08.01.3 - 08.13.2 - 02.13.5

ASTRONOMY
AND
ASTROPHYSICS
17.6.1996

Formation of PAHs, polyynes, and other macro-molecules in the photosphere of carbon stars

Christiane Helling[1,2], Uffe Gråe Jørgensen[1], Bertrand Plez[1], and Hollis R. Johnson[1,3]

[1] Niels Bohr Institute, University Observatory, Juliane Mariesvej 30, DK-2100 Copenhagen, Denmark
[2] Institute for Astrophysics and Astronomy, Technical University Berlin, Hardenbergstraße 36, D-10623 Berlin, Germany
[3] Astronomy Department SW 319, Indiana University, Bloomington, IN 47405, USA

Received date; accepted date

Abstract. Polycyclic Aromatic Hydrocarbons (PAH) have been suggested as a link in one of the possible routes from molecules to grains in carbon-rich stellar atmospheres. Carbon grains, except SiC, may form by conversion of C_2H_2 into PAHs. The most obvious site of this PAH production is the outer atmosphere of carbon stars. We present the first calculations of equilibrium partial pressures of PAHs and other complex carbon-bearing molecules in stellar photosphere models for carbon stars. We have included 38 atomic species and 338 molecules in chemical equilibrium. Our computed models have the following parameters: $T_{\rm eff}$=(2800K, 2600K, 2400K), Z=$Z_\odot$, log(g) ϵ [−1,0.5], C/O ϵ [1.1,7.0]. The results of the hydrostatic model calculations show that for atmospheric regions with T>1000K the partial pressures of PAHs and other large molecules are negligible small. This result is independent of the choice of fundamental stellar parameters.

For shallower depths than our hydrostatic photosphere models, however, a systematic chemical equilibrium exploration of the T-$P_{\rm gas}$ plane, Tϵ[750K,1000K], log$P_{\rm gas}$ ϵ[-5,3] ($P_{\rm gas}$ in dyn/cm^2), discloses PAHs as the species containing the largest fraction of carbon atoms not bound in CO for a range of temperatures around 850K. More carbon is contained in PAHs than in CO at these temperatures for C/O $\gtrsim$ 5.0.

Chemical equilibrium considered in a dynamical atmospheric structure confirms these results. The higher column density of PAHs is sufficient for the dynamic model to have an effect on the structure of the model (levitation) and on the emergent spectrum. However, some studies (Frenklach & Feigelson 1989) on kinetic PAH formation require a residence time at favourable T and $P_{\rm gas}$ which is longer than the time scales of realistic wind models. In the framework of our hydrostatic models we confirm that the conditions for PAH formation (T, $P_{\rm gas}$ or residence time) are not met, and we can point at the lower boundary condition needed for the wind models. Therefore either the observed dust grains form via other routes, or more complex stellar environments are required.

Key words: Stars: carbon - Stars: atmosphere - Stars: mass loss - molecular processes

1. Introduction

Observations indicate that the ratio between the mass of the dust and the mass of the gas in the outflow from carbon stars is $\dot{M}_{\rm d}$ / $\dot{M}_{\rm g}$ $\approx$ 4.5 $\times$ 10^{-3} (Knapp 1985; Jura 1986; Sedlmayr 1993). Since all oxygen is locked up into CO molecules in carbon stars, the grains that can form in carbon-rich stars are expected to be SiC, HAC (hydrogenated amorphous carbon), graphite, and diamonds. Carbon grains, except SiC (Cadwell et al. 1994), may form by conversion of C_2H_2 into PAHs (polycyclic aromatic hydrocarbon molecules) and further agglomeration into macroscopic grains. This idea is based on results of combustion experiments (Frenklach & Feigelson 1989, hereafter FF89) as well as on theoretical computations based on (1) classical nucleation theory (Keller & Sedlmayr 1983; Keller 1987; Gail & Sedlmayr 1987a) and (2) on chemical pathway analysis (Goeres 1993, hereafter G93). The agglomeration of PAHs leads to grains with crystalline or amorphous structures dependent on the combination of temperature and gas pressure conditions in the atmosphere (Gail & Sedlmayr 1984). The PAHs produced by analysis of chemical pathways tend to be more highly bent structures (due to minimalization of the entropy) than do the PAHs produced by combustion routes, and lead to maximum PAH nucleation rate at slightly lower temperatures (T $\approx$ 800 − 900 K; G93) than do combustion results (T $\approx$ 900 − 1100 K; FF89). Kinetic chemical reaction models (FF89; Cherchneff & Barker 1992, hereafter CB92) as

Send offprint requests to: Ch. Helling, email address: helling@nbi.dk

well as chemical pathway computations (G93) applied to the structure of wind models result, however, in a predicted formation of PAH molecules which is only a tiny fraction (by mass) of the mass of the observed amount of grains.

The questions these studies give rise to are therefore: Are the wind models substantially wrong ? Are the dust observations largely in error ? Are the grains in carbon stars only SiC ? Do carbon grains not form via PAH agglomeration ? Are the inputs (e.g. the photospheric, lower boundary condition) for the wind models in error ? Do the PAHs form already in the photosphere below the wind ? If not, where do they form in the atmosphere ?

To contribute to the solution of this dilemma we have computed a series of self-consistent photospheric carbon star models, where we include a large number of macro molecules in the chemical equilibrium computations. Our models are the first study of the formation of macro molecules in stellar photospheres, and they allow us to comment, in particular, directly on the three latter questions above. The model atmosphere code used is an updated version of the MARCS (Gustafsson et al. 1975, hereafter GBEN75) code, improved with extended chemical equilibrium computations, extensive cool-star opacities, spherical geometry, and an opacity sampling treatment of molecular opacities. The main strength of the photospheric computations, compared to the wind models, is a considerably better treatment of the radiative transfer, whereas the main weakness is the assumption of hydrostatic equilibrium. The photospheric models therefore surpass the wind models by performing a better prediction of the chemical equilibrium and the atmospheric structure in the deeper more dense layers, but are inferior to the wind models in the upper atmospheric layers where the dynamics may be active. The photospheric models therefore serve the double purpose (1) of giving a more reliable estimate of the possible PAH formation in the denser, lower atmospheric layers, and (2) of setting the lower boundary conditions for the wind models.

In addition, an expansion of our investigations to regions above the photosphere allows us to address the questions mentioned above to the full T-$P_{\rm gas}$ regime.

2. The yield of the wind models

In stellar atmospheres of solar metallicity, about 1% of the total mass is oxygen and about 0.5% is carbon (Anders & Grevesse 1989, hereafter AG89). In order to obtain the observed dust to gas ratio of $\approx 4.5 \times 10^{-3}$ (of carbon-rich dust) it is therefore necessary that this amount of carbon is transformed completely into grains. In stars with C/O<1 all the carbon is locked into CO molecules, and the large bonding energy (11.09 eV) of CO prevents it from participating in grain formation. At values of C/O>1 the fraction (by mass) of the gas that is transformed into dust via the C_2H_2−PAH route is given by

$$\frac{\dot{M}_{\rm d}}{\dot{M}_{\rm g}} = \frac{M_{\rm oxygen}}{M_{\rm total}} \times (C/O - 1) \times \eta_{\rm C2H2} \times \eta_{\rm grain} \qquad (1)$$

where $\eta_{\rm C_2H_2}$ is the mass fraction of carbon not bound in CO which becomes bound in C_2H_2 and $\eta_{\rm grain}$ is the mass fraction of the carbon initially in C_2H_2 which becomes transformed into grains (via the C_2H_2−PAH route). Our $\eta_{\rm grain}$ is basically what is called the yield, Y, in the works of FF89 and Cherchneff et al. 1992 (hereafter CBT92). The highest C/O ratio observed among the nearby bright carbon stars is 1.8 (Lambert et al. 1986, hereafter LGEH86). It is seen that for C/O $\approx$ 2, the observed $\dot{M}_{\rm d}$ / $\dot{M}_{\rm g} = 4.5 \times 10^{-3}$ can only be reached if both $\eta_{\rm C2H2}$ and $\eta_{\rm grain}$ are close to 100% ($\eta_{\rm C_2H_2} \times \eta_{\rm grain} = 0.6$ if C/O = 1.8 and $M_{\rm oxygen}$ / $M_{\rm total}$ = 0.01). In other words the formation of PAHs and following agglomeration into grains is required to be very efficient. In contrast to this, FF89 and CBT92 found yields (Y $\approx \eta_{\rm grain}$) of $\approx$ 0.01 or less when their kinetic reaction schemes were used with wind models.

FF89 studied time dependent PAH formation, with reaction rates based on a series of combustion analysis. They constructed simple analytical wind models, and followed the gas flowing with a constant velocity, v, until it reached layers of T = 700 K. The input parameters are $T_*(R_*)$, $\dot{M}$, v, H_2:CO:C_2H_2:HCN (with the ratio [C_2H_2/H_2] being the important ratio), and α being the slope in the assumed relation for the gas temperature as function of distance, r, from the centre of the star, $T(r) = T_*(R_*/r)^\alpha$. T_* and R_* are the "surface" temperature and radius (it is not clear what is meant by the "surface" but we assume it refers to $T_{\rm eff}$ and $R(T_{\rm eff})$, respectively, which is often called T_* and R_* in wind models, referring to a grey boundary condition). In their "standard" model, which leads to Y = 1.3%, they assume $T_* = 1500$ K, $R_* = 10^{14}$ cm, $\dot{M} = 10^{-4} M_\odot\,{\rm yr}^{-1}$, $v = 10\,{\rm m\,s}^{-1}$, [C_2H_2/H_2] = 10^{-4}, $\alpha = 0.5$. However, $T_{\rm eff} = 1500$ K is a very low value compared to observations (for example the brightest carbon stars in the solar vicinity have $T_{\rm eff} \epsilon$[2400 K; 3000 K] according to the work of LGEH86). The yield for stars of other effective temperatures can be estimated from the formulas (4) and (5) given by FF89, which leads to

$$\begin{aligned} Y_{T*}/Y_{T*=1500} &= (n_{T*}(r_{\rm cond})/n_{1500}(r_{\rm cond}))^{2.5} \\ &= \left(\frac{1500}{T_*}\right)^{5/\alpha}, \end{aligned} \qquad (2)$$

where $r_{\rm cond}$ is the distance from the centre of the star where the condensation is expected to take place. With $T_{\rm eff}$ = 2800K one gets $Y_{2800}/Y_{T*=1500} = 2 \times 10^{-3}$, or $Y_{2800} = 0.002\% \approx 0$. Even for the model which, in the computation of FF89, gives Y $\approx$ 50%, a corresponding scaling transforms the yield into $Y_{2800} = 0.1\% \approx 0$.

This model, having $R_* = 3 \times 10^{13}$ cm and otherwise the same input as the standard model, has the additional problem that the luminosity, $\log(L/L_\odot)=2\log(R/R_\odot) + 4\log(T_{\rm eff}/5770) = 3.0$, i.e. $M_{\rm bol} = -2.7$, is well below the observed lower luminosity limit of carbon stars. Westerlund et al. (1991) find that a reasonable lower limit for carbon stars in the Large Magellanic Cloud appears to be $M_{\rm bol} \approx -3.5$, and the models by Lattanzio (1986) and those of Boothroyd & Sackmann (1988) predict the first dredge up well above -2.7. Changing $T_{\rm eff}$ to 2800 K for this wind model brings the star into $M_{\rm bol} = -5.4$ in good agreement with observations, but again it leads to $Y_{2800} \approx 0$ as described above. In addition the choice of $v = 10$ m s^{-1} is low compared to the typical observed value $v_{\rm term} \approx 10$ km s^{-1}, which is also underlined by FF89 in noticing that when their analytical wind model was substituted with the self-consistent numerical model of Gail & Sedlmayr (1987b), their yield fell to $Y \approx 10^{-17}$ (≈ 0), mainly due to the more realistic velocity and corresponding shorter time allowed for the reaction chain from C_2H_2 to PAH. We finish this discussion of the pioneering models by FF89 by concluding that they produce $Y \approx 0$ for any realistic choice of stellar parameters.

CBT92 performed a similar study to the one by FF89, but reached even lower yields. They guided their choice of T versus $P_{\rm gas}$ structure by the numerical models due to Willson & Bowen (1986) and Bowen (1988). Even when increasing the density with a factor of two and lowering the velocity with a factor 3 (CBT92's standard model) compared to Bowen's standard model, they got a yield of $Y \approx 3 \times 10^{-10}$. Their model with the highest yield had $Y \approx 5 \times 10^{-5}$, and their model with an assumed photospheric boundary gas pressure more similar to our photospheric results, gave $Y \approx 5 \times 10^{-14}$ in the wind. Again the conclusion that $Y \approx 0$ in the wind was reached.

3. Method

3.1. Calculation of the Chemical Equilibrium

We use a version of Tsuji's program (1964) for chemical equilibrium calculations, considering 38 atoms and 338 molecules. The mixture of all species satisfies the condition of an ideal gas. No solids nor liquids are included. Elemental solar abundances are taken from AG89. We used as molecular data a combination of 314 of Tsuji's (1973, hereafter T73) and 24 of CB92's pressure-equilibrium constants for larger molecules not included in T73. When necessary, T73's equilibrium constants were updated for newer dissociation energies mostly from Huber & Herzberg (1979). The theory of a chemical equilibrium calculation is described in T73 and CB92. Following T73 we use the polynomial expression for the equilibrium constants

$$logK_p(\theta) = a_0 + a_1\theta + a_2\theta^2 + a_3\theta^3 + a_4\theta^4 \qquad (3)$$

with θ =5040K/T and a_i the fitting coefficients tabulated.

To test the data, we compared the pressure-equilibrium constants K_p from different data sources for the same molecule. We have done the calculations using data from T73, CB92 and Sauval & Tatum (1984, hereafter ST84, updated and kindly communicated to us by J. Sauval - private communication 1994). We compared every molecule (42 species) which was included in T73's data as well as in CB92. If ST84 contained the same molecule, we compared these 3 sources. T73 and ST84 data yield for every temperature T ϵ [1008K,5040K] very similar values for the pressure-equilibrium constant. CB92's data yield in some cases (CN, C_2N, C_3N, C_3, C_4H, C_4H_4, C_6H_6 - benzene, CS_2, SiC, SiO_2, SiC_2) different values from those of T73 and ST84. The largest differences occur for SiC_2, SiO_2, CS_2, C_6H_6 and CN. In addition, we were not able to reproduce CB92's results using their coefficients of the pressure-equilibrium constant.

Our updated Tsuji pressure-equilibrium constants supplemented by the data for 24 aromatic ring and complex molecules of CB92 (C_5, C_6H, C_4H_6, C_6H_2, C_6H_4 - benzyne, $C_{10}H_7$ - naphtyl, HC_5N, HC_7N, HC_9N, $HC_{11}N$, C_4H_4S - thiophene, C_4H_4O - furan, C_5H_5N - pyridine, C_6H_5O - phenoxy, C_6H_6O - phenol, $C_{10}H_8$ - naphtalene, $C_{10}H_{16}$ - adamantane, $C_{14}H_{10}$ - anthracene, $C_{14}H_{10}$ - phenanthrene, $C_{18}H_{12}$ - triphenylene, $C_{18}H_{12}$ - benzo(c)phenanthrene, $C_{22}H_{14}$ - benzo(c)chrysene, $C_{24}H_{12}$ - coronene, $C_{106}H_{56}$) yield partial pressures for most species very close to CB92's results. We found in later calculations using the MARCS code an agreement between partial pressures calculated with our chosen set of pressure-equilibrium constants and partial pressures calculated using molecular data given by Irwin (1981).

For convenience in presenting the results, we will not mention all molecules used in the chemical equilibrium calculation, but only the molecules of interest. Furthermore, the molecules considered are grouped according to their structure as follows: (1) large N-bearing species HC_xN, (2) complex hydrocarbon species C_xH_2, (3) CH-bearing radicals C_xH, CH_x and (4) C_x.

3.2. Calculation of the Model Photosphere

The model atmosphere program used is the MARCS program (GBEN75) in an improved and updated version for cool C-star atmospheres (Jørgensen et al. 1992) combined with the chemical equilibrium routine written by Tsuji (1964) and improved by us to include formation of PAHs, polyynes and other macro molecules in gas phase. We do not investigate any transition to a solid phase.

The MARCS code yields the hydrostatic structure of a stellar atmosphere for given effective temperature $T_{\rm eff}$, surface gravity g, C/O ratio, and metallicity Z. As an integrated part of the computation of the model structure we also calculate the partial pressures of all molecules using the above mentioned equilibrium routine.

We present here model calculations for various combinations of the parameters log(g) ϵ [-1,0.5] and C/O ϵ [1.1,7.0], $T_{\rm eff}$=(2800K, 2600K, 2400K), keeping Z=Z$_\odot$.

All hydrostatic models are computed from the Rosseland optical depth $\log(\tau_{\rm Ross})$=2.0 (bottom of the atmosphere, inner boundary) to $\log(\tau_{\rm Ross})\lesssim-6.1$ (the "surface" layer, outer boundary). At lower optical depth the hydrostatic assumption become unjustifiable. The step width used, or the thickness of the so defined atmospheric layers, is $\Delta\log(\tau_{\rm Ross})$=0.15.

Opacities from CO, CN, C_2H_2, C_2 and HCN are included. Data for CO and C_2 are from the work of Querci et al. (1974), data for CN from Jørgensen & Larsson (1990), data for HCN from Jørgensen et al. (1985) and data for C_2H_2 from Jørgensen (1982, unpublished). The molecular opacities were treated in the opacity sampling (OS) approximation at 5365 wavelengths from 1250$\AA$ to 25μm.

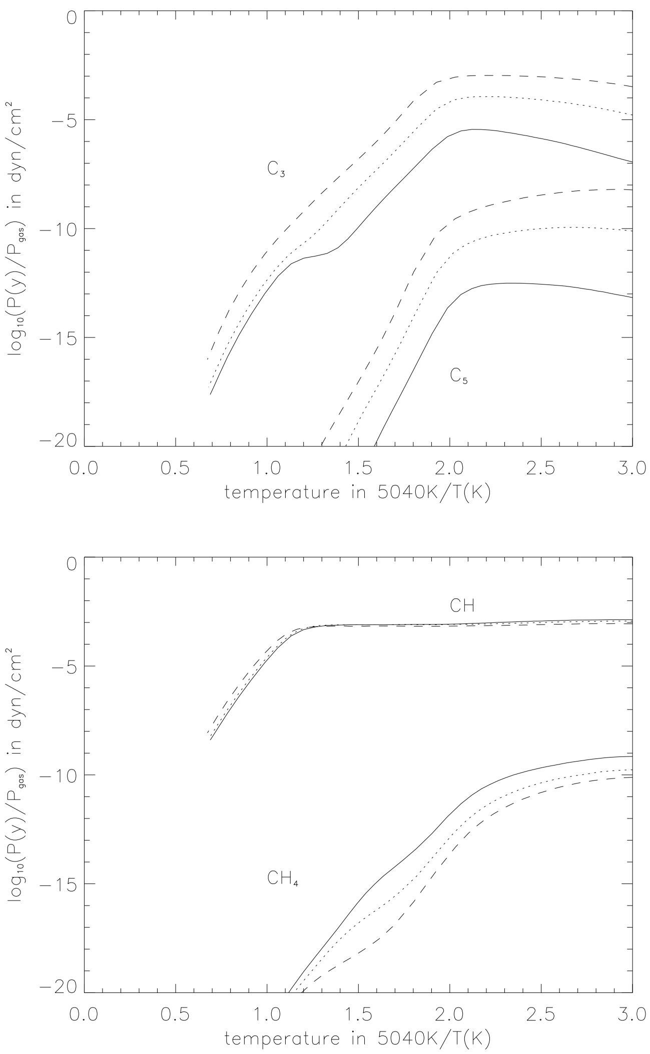

Fig. 1. The influence of the C/O ratio on the ratio $P_y = P(y)/P_{\rm gas}$ at $T_{\rm eff}$=2800K and a surface gravity log(g)=0.5. The line stiles denote the following C/O ratios investigated: solid = 1.1, dotted = 1.8, dashed = 7.0.

4. Results and Discussion

4.1. MARCS Model Photospheres

One of the main result of our analysis of the carbon star photosphere is that molecules much more complex than usually considered in the computation of photospheres do form already at temperatures well above 1000K, although in very small amounts. The molecules which appear with a partial pressure $P(y) > 10^{-20}$dyn/cm^2 at $\log(\tau_{\rm Ross})\geq -6$ do not include any PAHs, but do include small complex hydro-carbon molecules as well as polyynes. We notice in particular the existence of the following species: HC_xN with x=2n+1 and C_xH_2 with x=2n for n=0,...,3 , C_xH x=2,...,5, C_x for x=2,...,6 and CH_x for x=2, 3, 4. The absolute amount of the molecules depends on surface gravity and C/O-ratio as well as on $T_{\rm eff}$ of the model.

4.1.1. Influence of Surface Gravity on the Partial Pressures

Tests with $T_{\rm eff}$=2800K (T$\gtrsim$1500K), C/O=1.1 and log(g)ϵ[-0.5,0.5] show that surface gravity affects the amount of a formed molecule only slightly.

A change in gravity means the same change in gas pressure for all temperatures considered. Therefore, increasing surface gravity increases the absolute amount of the partial pressure for all the molecules considered.

4.1.2. Influence of C/O-ratio on the Partial Pressures

We used the same model parameters as mentioned above: $T_{\rm eff}$=2800K (T$\gtrsim$1500K), log(g)ϵ[-0.5,0.5], but C/Oϵ[1.1, 7.0].

The amount of carbon available for molecules other than CO increases by a factor of 8 when the C/O ratio grows from 1.1 to 1.8. It goes up again with a slightly lower factor of 7.5 when the C/O ratio increases from 1.8 to 7.0 (see Fig. 1 and 2).

The partial pressure of the complex molecules varies with the amount of carbon not bound in CO. An increased amount of available carbon produces higher partial pressures for open-shell species (C_x, C_xH), cyanopolyynes (HC_xN), and C_6H_2, whereas the partial pressure for other species like C_xH_2 and CH_x decreases (see also Table 1). The results do not depend on the surface gravity. In every case, the smallest member of a group (C_2, C_2H, HCN, C_2H_2, CH_2) is the most abundant.

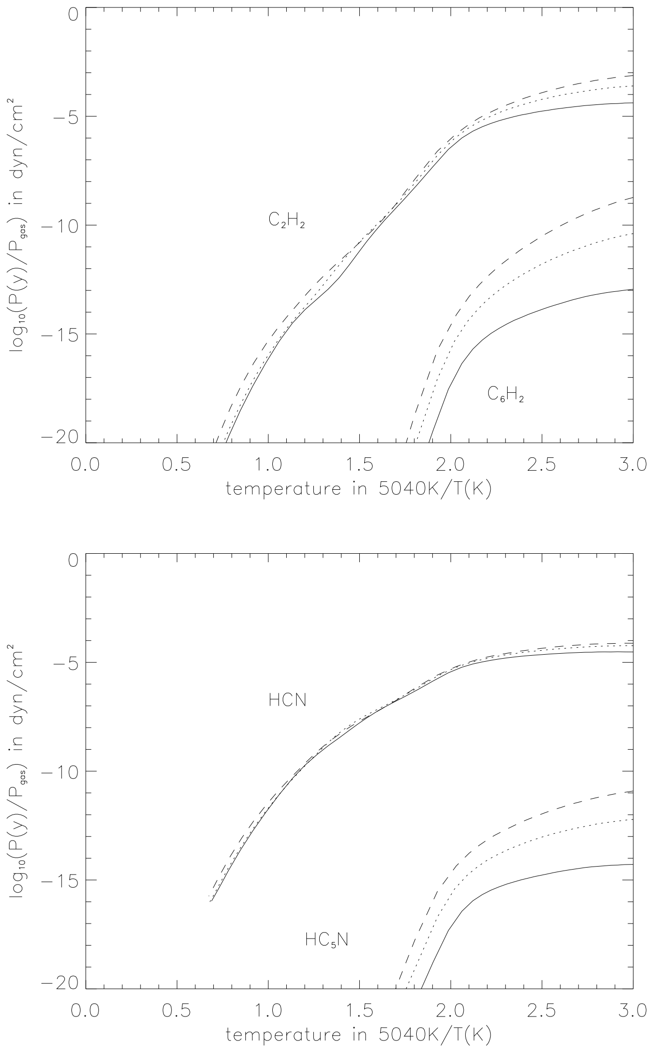

Fig. 2. Same as Fig. 1 but for different species.

Table 1. Behaviour of the ratio $P(y)/P_{\rm gas}$ of various species y for an increase of the C/O ratio from 1.1 to 7.0.

Species y	
C_x, x= 2 . . . 5	increase
CH	increase until $\theta \approx 1$
	slight decrease for $\theta > 1$
C_xH, x= 2 . . . 6	increase
$HC_{2n+1}N$, n= 0 . . . 3	increase
C_xH_2, x= 2, 6	increase
CH_2	vary
CH_x, x= 3, 4	decrease
CN	increase
CS	increase
CS_2	decrease
C_6H_2	increase

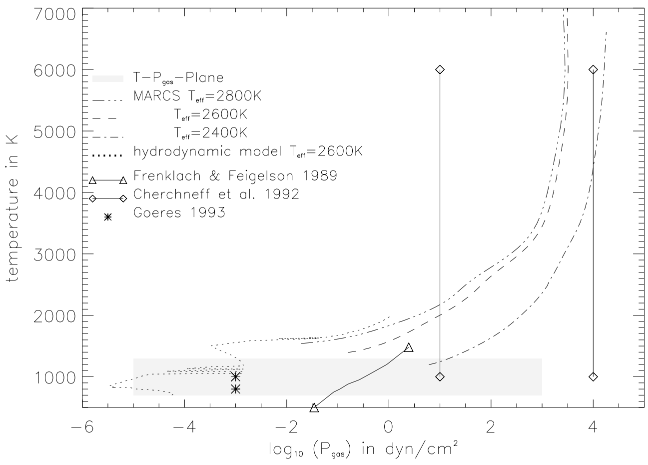

Fig. 3. T-$P_{\rm gas}$ profiles and points explored by previous works and the present one. The shaded area has been systematically explored by us (see text). The hydrostatic MARCS models are shown for C/O=1.1 and log(g)=0, the dynamic model for C/O=1.8 and log(g)=−1

4.1.3. Influence of $T_{\rm eff}$ on the Partial Pressures

We calculated stellar atmosphere models with lower effective temperatures than 2800K in order to study the effect of decreased temperatures in the shallowest layers on complex molecules in the gaseous phase in chemical equilibrium. We calculated models with $T_{\rm eff}$=2600K (T$\gtrsim$1400K) and $T_{\rm eff}$=2400K (T$\gtrsim$1200K) for C/O=1.1 and log(g)=0. The calculations confirm our above mentioned results. Even in models where the temperature of the shallowest layer becomes lower than 1200K, we do not find larger molecules than HC_7N and C_6H_2.

As seen in Fig. 3, a decreasing effective temperature yields an increasing gas pressure at a given temperature in the atmosphere, and, hence, increased partial pressures of the species as well.

That fact in mind, we investigated the ratio $P_y = P(y)/P_{\rm gas}$, of the partial pressure of the species y to the gas pressure for HC_xN, C_xH_2, C_xH, C_x, CH_x and SiC_2 for typical temperatures of a MARCS model. P_{C_xH} (x=4,5,6) and P_{C_x} (x=2...5) increase with decreasing gas pressure in shallower layers with low temperatures. On the other hand, $P_{C_xH_2}$ and P_{HC_xN} decrease with decreasing gas pressure (e.g. T=1400K, see Fig. 4). Open-shell species (radicals as C_xH and C_x) seem to form more easy under low gas pressure and high temperature than closed-shell species (as C_xH_2 and HC_xN). The radicals are more stable under these conditions, although open-shell species are extremely reactive and have a very short lifetime under terrestrial conditions. The effect is very much dependent on the temperature of the atmospheric layer, as shown by calculations for a given temperature and varying gas pressure using Tsuji's chemical equilibrium routine. For a higher temperature (e.g. T=2400K, see Fig. 5) the ratio P_y of the complex molecules y decreases with decreasing gas pressure for all molecules considered, and the closed-shell species become more stable than the open-shell species.

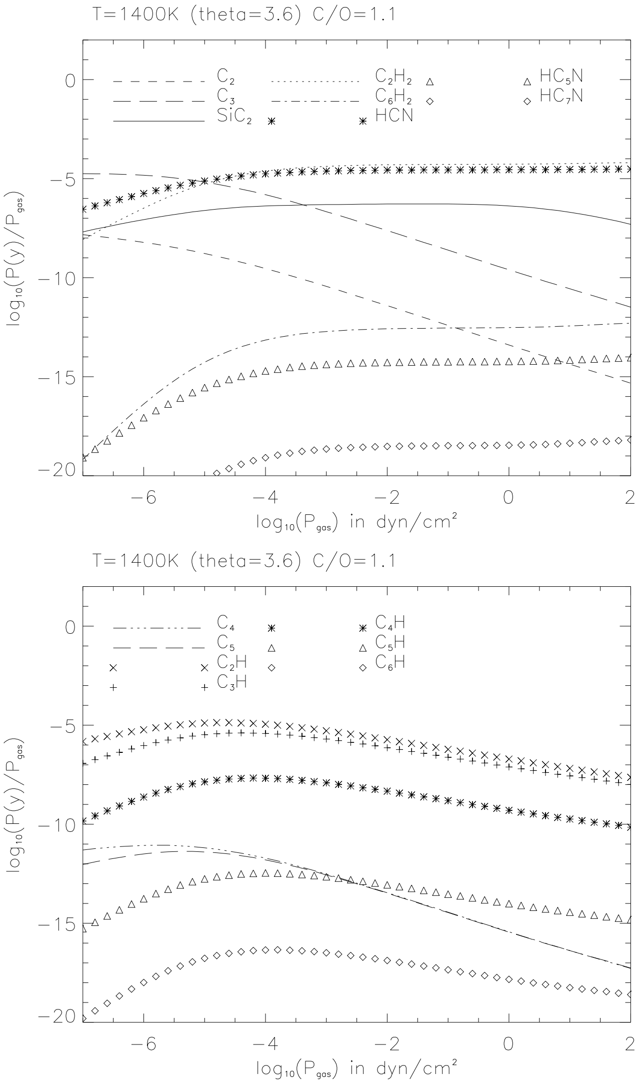

Fig. 4. Chemical equilibrium calculation using a constant temperature T=1400K and varying the gas pressure P_{gas}

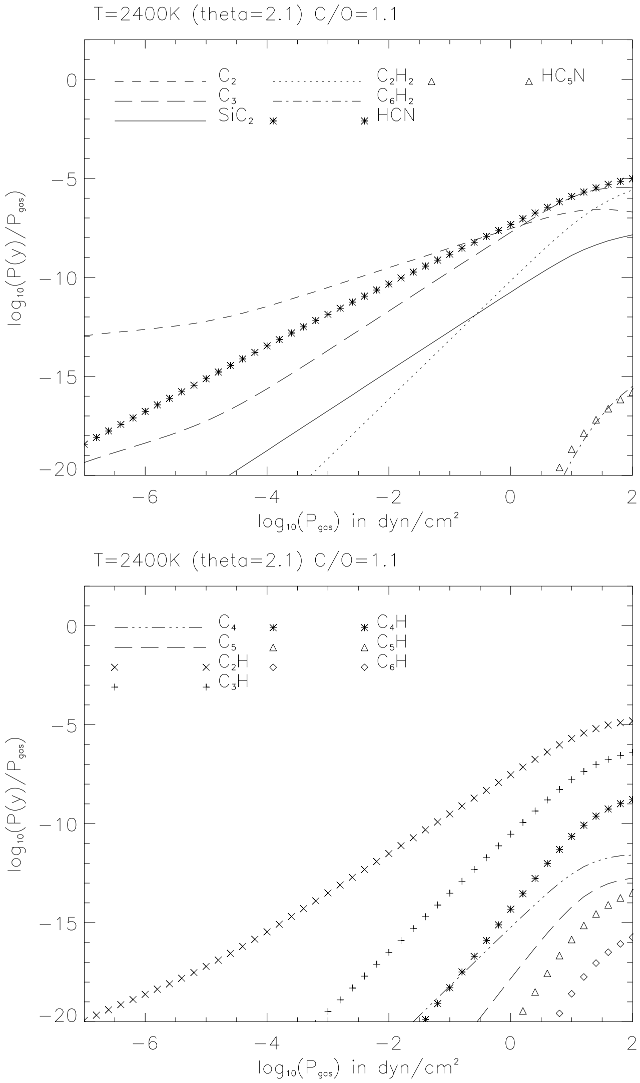

Fig. 5. Chemical equilibrium calculation using a constant temperature T=2400K and varying the gas pressure P_{gas}

4.2. Other Model Calculations

Our self-consistent stellar atmospheric models are calculated assuming hydrostatic equilibrium. Dynamically calculated stellar atmospheres are much more extended. They have higher pressure at a given height in the outer atmosphere, and much larger column density than static models. We may thus expect an easier formation and hence, higher equilibrium concentrations of larger complex molecules.

We examine the situation in a typical dynamically calculated atmospheric T-P_{gas} structure of the Berlin group (for more details about these models see e.g. Fleischer et al. 1992) kindly provided to us by A.Fleischer ($T_{\rm eff}$=2600K, M=$M_\odot$, L=$10^4 L_\odot$, C/O=1.8, log(g)= -1, $\dot{M}=10^{-5} M_\odot$/yr). We performed molecular equilibrium computations for a number of (T,P_{gas}) values of this model structure, and compare here the results with our self-consistent computations of molecular equilibrium calculations with a MARCS model with the same parameters ($T_{\rm eff}$=2600K, C/O=1.8, log(g)= -1).

Although the dynamical model extend to much lower gas pressures (and the hydrostatic to much higher gas pressures), the T-P_{gas} structures of the dynamical and the corresponding hydrostatic model are quite similar to one another in the region of overlap. The same molecular species are therefore formed in about the same amount, in the overlap-region of the two models. A given (T,P_{gas}) point in two models does, however, not correspond to the same geometrical position in the two models, and the dynamical model is considerably more extended than the hydrostatic one. For example, $R(T=1500K)_{dynamic}/R(T=1500K)_{static}=1.9$. It is not clear yet how large a fraction of this difference should be ascribed to the lack of dynamics in the MARCS models, and how much should be ascribed to the simplified radiative transfer treatment in the dynamic models. Far from the star, however, the dynamic models are consistent with the observed mass loss and the requirement of mass conservation, whereas extrapolation of hydrostatic models are not (Johnson 1991).

The dynamic model yields a larger column density in the temperature range of the static model, and hence, a higher production of larger molecules in number. But the ratio n(large molecules)/n(H_2) is left unchanged, in the range where the two models overlap.

In the outer part of the dynamic model, the temperature drops to levels not reached by the MARCS model, with still an appreciable gas pressure. In Fig. 6, we plot the fraction F_y of carbon atoms bound in a species y along the temperature profile for T≤1000K in the Berlin model. As C/O=1.8, F_y(CO)=1/1.8. At temperatures higher than 850K, most of the remaining 45% of carbon is bound in C_2H_2. HCN contains 1% or 2% of the total amount of carbon. SiC_2 and Si_2C are the only important Si-bearing molecules and sum to less than 1% of the total amount of carbon available.

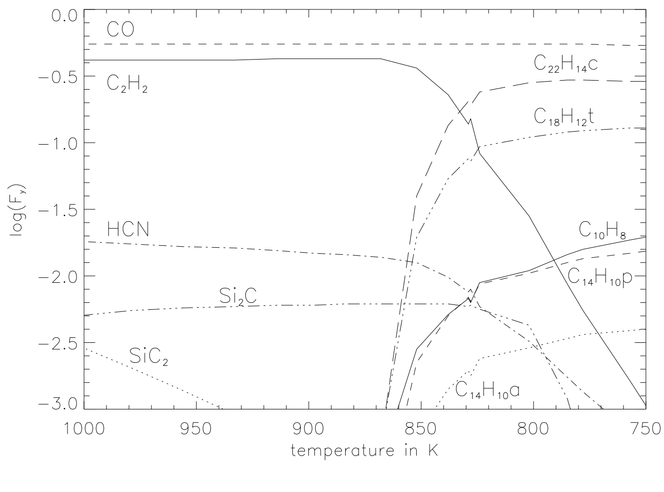

Fig. 6. Fraction F_y of carbon in species y ($C_{14}H_{10}$a = anthracene, $C_{14}H_{10}$b = phenanthrene, $C_{18}H_{12}$t = triphenylene, $C_{22}H_{14}$c = benzo(c)chrysene) in the outer layers of the Berlin hydrodynamic model of Fig. 3, (C/O=1.8), computed with our chemical equilibrium routine. Below T≈850K basically all the carbon not in CO is bound in PAH molecules, whereas it is bound in much smaller molecules (mainly C_2H2) at temperatures above 850K.

Below 850K, carbon which at higher temperatures was bound in C_2H_2 is transferred into large PAH molecules. The partial pressure will be larger than that from C_2H_2 for T≤850K. The concentration of PAHs increases significantly. Large PAH molecules such as $C_{22}H_{14}$-benzo(c)chrysene, rapidly dominate over smaller PAHs and hydro-carbon molecules such as C_6H_2 when the temperature decreases further.

Our calculation presents, however, some limitations: The polynomial expansions we utilize for the chemical equilibrium constants, K_p, were optimized for 1000K<T<6000K. We have checked though, that within the region 600K<T<1000K where we use them, their variation is smooth and shows no suspicious oscillations.

The relative partial pressures of the various PAHs are sensitive to uncertainties in the values of the K_p's, and the accumulated uncertainty can grow quite large for the largest PAHs (Stein & Fahr 1985). The anonymous referee to the present paper pointed out that results from combustion experiments indicate that the K_p values we are using from the work of CB92 might be substantially in error in particular for the important PAH molecule coronene. The conditions at the high pressures and the relative simple gas-mixtures in combustion experiments are, however, quite different from the complex low pressure conditions in a stellar atmosphere or wind, and too definite conclusions should therefore not be drawn from such comparisons. Independent of whether such changes in the relative abundances of the various PAHs may exist, the sum of the partial pressures of all the PAH molecules are quite robust toward uncertainties in the K_p values, and clearly the sum of the PAHs substitute C_2H_2 as the main carbon bearing molecule (after CO) at temperatures below 850K in the chemical equilibrium computations illustrated in Fig. 6.

A more severe limitation is the requirement of chemical equilibrium, which allows an infinite time of formation for all species. A look at the wind model shows that around T=850K, the velocity is about 15km s^{-1}. The residence time in a region considered in 800K≤T≤900K (∼1.5R_*) is then Δt∼3.5 × 10^7s. FF89 estimate a necessary residence time of about 10^{11}s (≈3200 yr), which could be obtained if the velocity was only ∼5m s^{-1}. The same conclusion was reached in the time dependent PAH formation models by FF89 and CBT92 who found negligible quantities of PAHs to form when various wind models were adopted as a (fixed) structure for their condensation models (see section 2). If the grains that drive the mass loss in these models indeed condense from PAHs, one must then allow for PAHs to form first. As is seen from Fig. 7, 8 and 9 most of the carbon (not bound in CO) is bound in PAHs for low temperatures and low gas pressures. For higher temperatures C_2H_2 is the dominating carbon molecule, whereas CH_4 dominates at low temperatures and high pressures. For increasing C/O ratios the PAH dominated region of the T-P_{gas} plane expands to higher temperatures and pressures (see next subsection). Hence, the gas must be allowed to cool down to about 850K and stay at this temperature for a long enough time.

We can derive a rough residence time around 800K in a typical wind of a carbon star. From the mass conservation equation ($\dot{M}$ =4πR^{2}ρv) and the ideal gas law (P_{gas}=nkT) we estimate in convenient units:

$$v \approx \frac{\dot{M}_{-6} T_{800}}{R^2_{300} P_{\rm gas}} \times 4\ ms^{-1} \tag{4}$$

where v is the velocity of the wind, $\dot{M}_{-6}$ the mass loss in units of 10^{-6}M$_\odot$yr^{-1}, T_{800} the temperature T/800K, R_{300} the radius in units of 300R$_\odot$ and P_{gas} the gas pressure in dyn cm^{-2}.

Assuming that the gas stays at favourable temperatures for about a 1R$_*$ travel, the residence time Δt is then roughly:

$$\Delta t \approx \frac{R^3_{300} P_{\rm gas}}{\dot{M}_{-6} T_{800}} \times 5 \times 10^{10} s \tag{5}$$

or alternatively

$$\Delta t \approx \frac{R^3_{300}}{\dot{M}_{-6}} \rho_{-10} \times 1.6 \times 10^{11} s \tag{6}$$

where ρ_{-10} is the density in units of 10^{-10}g cm^{-3}. In typical numerical models , Δt≤10^8s. It is worth noting that the residence time could be greatly increased if the PAHs were cooler than the gas. The thermal decoupling of the PAHs and the gas (G93) might occur due to an inverse greenhouse effect (Cherchneff et al. 1991).

Cadwell el al. 1994 (hereafter CWFF94) consider induced nucleation as the likely mode of grain formation. The basic idea is carbon deposition on pre-existing solid surfaces of seeds. From laboratory works (Carmer & Frenklach 1989) and analyses of meteorites (Lewis et al. 1990; Gallino et al. 1990; Clayton et al. 1991) condensed SiC is considered a likely candidate for seeds. CWFF94 suggest grain growth by deposition of C_2H_2 molecules for high temperatures, and in cooler regions any present gas-phase PAHs may stick to the grain. CWFF94 explain the existence of PAHs in planetary nebulae as due to desorption of the ejected grains containing PAHs from ultraviolet radiation, sputtering, or shattering by grain-grain collision. Their considerations assume the existence of enough condensed SiC seeds. However, the ratio of Si to C in carbon stars as well as the ratio of stellar SiC grains to pure carbon grains (diamonds) in meteorites is very small. The individual meteoritic SiC grains are very big compared to the diamonds. CWFF94's large grains result from a very low outflow velocity ~0.01km s^{-1} (see section 2). Only homogeneous stellar grains are found in the meteorites (Anders & Zinner 1993) which, in the scenario of CWFF94, would require that the carbonous coating of the SiC grains is completely destroyed after the formation and before incorporation in the meteorites.

4.3. Extrapolation of the Photospheric Structure

PAHs only form in small amounts in our MARCS atmosphere models. None of them reach P_y >10^{-27} , only C_6H_2 reaches $P_{C_6H_2}$ ~10^{-10} in the outermost layers of the models. The extension of the computation of these models to shallower optical depth, and thus lower temperatures, was not possible because of numerical difficulties. We instead explored the T-P_{gas} plane systematically for T ϵ [750K,1300K] and log P_{gas} ϵ [−5,3] (P_{gas} in dyn/cm^2). Fig. 7, 8 and 9 show the dominant species at chemical equilibrium in this regime.

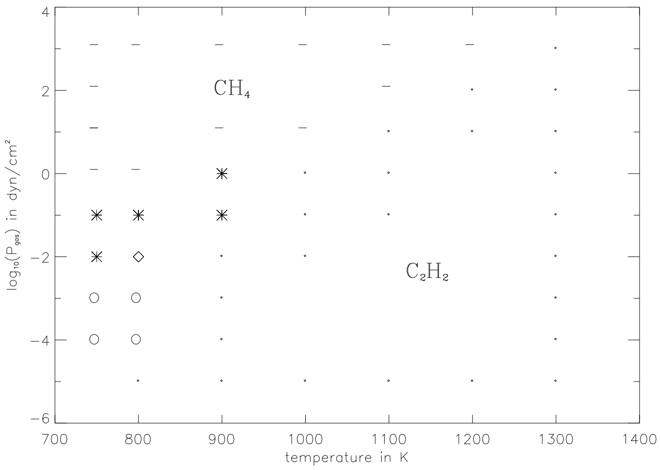

Fig. 7. Molecules accounting for the largest fraction of C not bound in CO at equilibrium in the T-P_{gas} plane. In all cases the fraction is larger than 10%. Note that PAHs do also appear in smaller amounts outside the region where they dominate. The symbols relate to the following PAHs at C/O=1.1: asterisks = $C_{10}H_8$, diamond symbol = $C_{18}H_{12}$t (triphenyle), circles = $C_{22}H_{14}$c (benzo(c)chrysene). The minus sign covers the CH_4 dominated region, and the dot covers the C_2H_2 dominated region.

For each (T,P_{gas}) point is shown the most abundant PAH containing at least 10% of the carbon not bound in CO. In many cases 2 or 3 PAH species represent each more than 10% of the "free" carbon. When no single PAH accounts for more than 10% of the free carbon, the most abundant molecule after CO is shown. Note that in the C/O=5.0 case, CO is not the most abundant species, as it contains at most 20% of all carbon, although the PAHs have still very low partial pressures.

Inspection of Fig. 7 − 9 shows that C_2H_2 dominates (after CO) at lower pressures and higher temperatures. Our MARCS models fall in the C_2H_2-dominated region. At high pressures and lower temperatures CH_4 is the main species after CO (brown dwarf and planetary regime). Tsuji noted this in 1964, and CB92 confirmed his result only for low C/O ratios (but larger than 1).

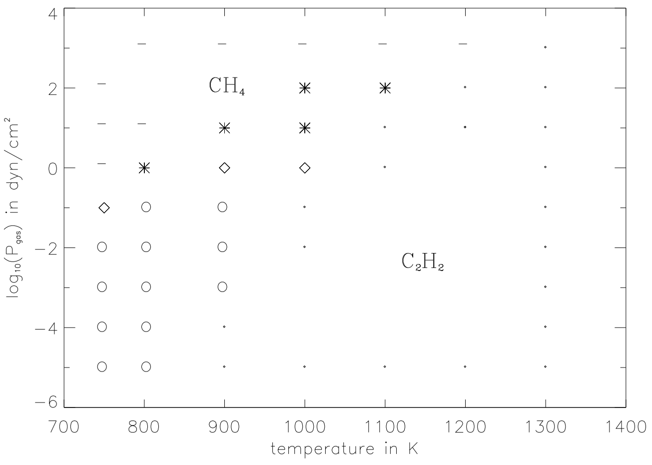

Fig. 8. Same as Fig. 7 for C/O=1.8

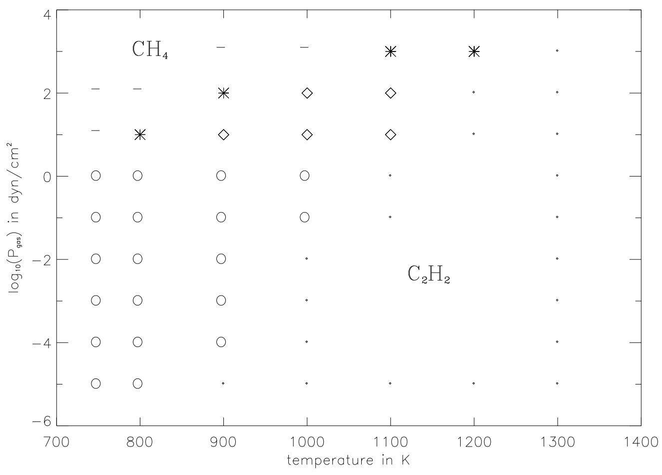

Fig. 9. Same as Fig. 7 for C/O=5.0

Small PAHs appear above the 10% level for higher and higher T and P_{gas} for increasing C/O ratio. Larger PAHs appear at slightly lower T and P_{gas}. PAHs totally dominate for most pressures for T$\leq$900K (higher for C/O=5.0).

Around 800K, most of the carbon not bound in CO goes into PAHs. PAHs are also formed at lower levels, outside the region of the Fig. 7, 8 and 9 where they stand out.

As discussed in the previous section, the main limitation of these calculations is the assumption of chemical equilibrium. To produce efficiently these large molecules requires a long residence time of the gas in a favourable region of the T-P_{gas} plane of Fig. 7 − 9. Our investigation localizes the T-P_{gas} region where PAHs will form, provided the gas is given sufficient time here. Any model atmosphere code that considers carbon grains agglomerating from PAHs in gas phase should as a minimum requirement include layers with a combination of (T, P_{gas}) from this region.

Extrapolations to lower optical depths of our static models will have too low pressures, hence the pressure needs to be increased in the low T layers. Pulsations and shock waves may help. Levitation of the gas by radiation pressure on molecular lines has a similar effect. However, it is included in our models, and C_2H_2 and HCN, the major actors, only have a limited effect. We discuss levitation further in the next section.

4.4. Levitational Effects and Mass Loss

Mass loss through a wind seems to be a common feature of red-giant stars, but the mechanisms are not well understood. While the high mass loss rate in Mira variable stars (10^{-6} $M_\odot$ yr^{-1} to 10^{-4} $M_\odot$ yr^{-1}), including carbon Miras, seems to be driven by radiative force on grains, with the star perhaps being first distended by its enormous pulsational energy and momentum, the same certainty does not exist for non-Mira stars. However, theoretical considerations set a lower limit for dust-driven mass loss ($\sim$ few 10^{-7} $M_\odot$ yr^{-1}), and some red-giants are observed to have lower mass-loss rates than this limit. Furthermore, many M and C giant stars show no evidence of excess infrared emission due to dust. Without grain formation, there exists a serious deficiency of a mechanism for driving a wind in these stars.

A likely candidate for driving the wind of mass losing red giants without grains is radiative force on molecules (Maciel 1976, and see Gustafsson & Plez 1992 for a review, hereafter GP92). However, attractive as this possibility seems, calculations to the present (GP92, Jørgensen & Johnson 1992) find the radiative acceleration on the molecules studied (i.e., H_2O, C_2H_2, HCN and C_3) to be at most a few percent of the gravitational acceleration. Additional molecular absorption could increase the radiative force.

Can PAHs and complex hydro-carbon molecules increase the absorption significantly? To do so would require an optical depth in the absorber of at least ~ 0.001. With an integrated absorption coefficient of a typical PAH − pyrene ($C_{16}H_{10}$) − of $\approx 10^{-17}$ cm per molecule in the IR (Joblin et al. 1994), this would require a column density of $\sim 10^{15}$ particles per cm^2.

The integrated absorption coefficient of HCN (or C_2H_2 or C_3) in the near IR region is of the same order as that of a typical PAH molecule. The radiative acceleration may be expressed as:

$$a_{\rm rad} = \frac{4\pi}{c\rho(y)} \int \chi_\nu(y) H_\nu d\nu \qquad (7)$$

with H_ν the monochromatic radiative flux, $\chi_\nu(y)$ the opacity in cm^{-1}, and $\rho(y)$ the density of the species y. $\chi_\nu(y)$ is proportional to $P(y)$. For two molecules of comparable integrated absorption coefficient (here HCN and

C_6H_2), the ratio of the radiative force on the atmosphere is therefore proportional to the ratio of their partial pressures. Since this ratio $P(C_6H_2)/P(HCN) \approx 10^{-8}$ in the photosphere we conclude that the radiative force on C_6H_2 in the photosphere is negligible compared to the radiative force on HCN. Since C_6H_2 has the highest pressure among the complex molecules at the photospheric temperature (T $\geq$ 1500K) considered in the present investigations with the MARCS code, we conclude that complex molecules and aromatic ring molecules are unable to levitate the atmosphere or initiate the stellar wind at these photospheric depths in our static models.

However, investigations of the column densities in a typical comparable dynamical model (see section 4.3) yield an approximate monochromatic optical depths of 0.02 for $C_{10}H_8$ and 0.17 for $C_{22}H_{14}$, assuming a cross section of 10^{-18} cm^2 per one of these molecules. Thus, if PAHs would have enough time to form (or form via carbon deposition on seeds, inverse greenhouse effect or other mechanisms which might increase their abundances) in a dynamic model atmosphere they would have a strong effect on the atmospheric structure (levitation) and the emergent spectrum, and therefore should be included self-consistently in the wind models.

5. Conclusions

We calculated equilibrium concentrations of a variety of complex molecules and PAHs in carbon-rich atmospheric mixtures.

1. In hydrostatic MARCS model photospheres with $T_{\rm eff}$ ϵ [2400K, 2800K], PAHs have only very low abundances. Open-shell species can form under low gas pressure and high temperature with abundances comparable to that of C_6H_2. The largest complex hydro-carbon molecule that appears in a significant amount is C_6H_2 ($\sim 10^{-10} \times P_{\rm gas}$). PAHs are thus found to have no effect on the structure and will not produce spectral features in such models.
2. Equilibrium calculations for (T,$P_{\rm gas}$) values corresponding to a dynamical stellar atmosphere model show large concentrations of PAHs in the layers with T$\leq$850K. In that case, the column densities are high and optical depths close to unity can be expected in the bands where these molecules absorb. Levitational effects might be important and the spectra will be affected.
3. A systematic extrapolation of the T-$P_{\rm gas}$ plane at temperatures down to 750K shows that in equilibrium PAHs bind a large fraction of the available carbon ($\geq$10% of the C not bound in CO) in a range of gas pressures for low temperatures (as seen in Fig. $7-9$). However, the hydrostatic models never reach this region of the T-$P_{\rm gas}$ plane, and in the hydrodynamic models the gas flows too rapidly through this region to allow PAH formation.
4. The main limitation of our calculations lies in the assumption of chemical equilibrium. Chemical reaction studies (FF89, CBT92) found that the required residence time around 800K for the formation of PAHs is much larger than allowed in the wind and atmosphere models presented. If such large residence times are really needed, then either (1) dust grains in carbon stars do not form via PAHs as suggested in several previous studies, or (2) much more complex structures for the upper atmosphere of carbon stars (for example, hotter and cooler regions) than in one-dimensional photosphere and wind models are required. Such models would need to predict a substantially higher gas pressure in the temperature range around T=700-900K than existing models, if the PAHs condense out of the gas phase and agglomerate to form the observed dust in carbon stars.

Acknowledgements

We are thankful to T.Tsuji for providing us with a copy of his chemical equilibrium routine, to A.J. Sauval for sending us an electronic version of his updated set of molecular dissociation constants, and A. Fleischer for providing us with an unpublished dynamical model for comparison with our hydrostatic models. B.Plez acknowledges support by a HCM grant from the commission of the European communities. Ch. Helling acknowledges an ERASMUS fellowship from the TU Berlin.

References

Anders, E. & Grevesse, N. 1989, *Geochimica et Cosmochimica*, 53, 197
Anders, E. & Zinner, E. 1993, *Meteoritics*, 28, 490
Boothroyd, A.I., Sackmann, I.-J., 1988, *ApJ*, 328,641
Bowen, G.H., 1988, *ApJ*, 329, 299
Cadwell, B.J., Wang, H., Feigelson, E.D., Frenklach, M. 1994, *ApJ*, 429, 285
Carmer, C., Frenklach, M. 1989, *Appl.Phys.Lett.*, 54, 1430
Cherchneff, I., Barker, J. R. 1992, *ApJ*, 394, 703
Cherchneff, I., Barker, J., Tielens, A. 1991, *ApJ*, 377, 541
Cherchneff, I., Barker, J., Tielens, A. 1992, *ApJ*, 401, 269
Clayton, D.D., Obradovic, M., Guha, S., Brown, L.E 1991, *Lunar Planet.Sci*, 22, 221
Fleischer, A.J., Gauger, A., Sedlmayr, E. 1992, *A&A*, 266, 321
Frenklach, M., Feigelson, E.D. 1989, *ApJ*, 341, 372
Frenklach, M., Carmer, C.S., Feigelson, E.D. 1989, Nat, 339, 196
Gail, H.-P., Sedlmayr, E. 1984, *A&A*, 132, 163
Gail, H.-P., Sedlmayr, E. 1987a, in *Physical Processes in Interstellar Clouds*, ed. Morfill, G.E. and Scholer, M., Dortrecht, Reidel, 275
Gail, H.-P., Sedlmayr, E. 1987b, *Astr.Ap.*, 171, 197
Gallino, R., Busso, M., Picchio, G., Raiteri, C.M. 1990, *Nat*, 348, 298
Gustafsson, B., Bell, R.A., Eriksson, K., Nordlund, Å. 1975, *A&A*, 42, 407
Gustafsson, B., Plez, B. 1992, in *Instabilities in evolved super- and hypergiants*, ed. de Jager C., Nieuwenhuijzen A., North Holland, Amsterdam, 86

Goeres A. 1993, in *Rev.mod.Astr.*, ed. Klare G., 6, 164
Huber, G., Herzberg, K. P. 1979, *Molecular spectra and molecular structure, IV Constants of diatomic molecules*, van Nostrand Reinhold Company, New-York
Irwin, A. W. 1981,*ApJSS*, 45, 621
Jura, M. 1986, *ApJ*, 303, 327
Joblin, C., d'Hendecourt, L., Léger, A., Défourneau, D. 1994, *A&A*, 281, 923
Johnson, H. R. 1991, *A&A*, 249, 455
Jørgensen, U. G., Almlöf, J., Gustafsson, B., Larsson, M., Siegbahn, P. 1985, *J. Chem. Phys.*, 83, 3034
Jørgensen, U. G., Larsson, M. 1990, *A&A*, 238, 424
Jørgensen, U. G., Johnson, H. R., Nordlund, Å. 1992, *A&A*, 261, 263
Jørgensen, U. G., Johnson, H. R. 1992, *A&A*, 265, 168
Knapp, G. R. 1985, *ApJ*, 293, 273
Keller, R., Sedlmayr, E., 1983, *Mitt.d.Astr.Ges.*, 60, 312
Keller, R., 1987, in *Polycyclic Aromatic Hydrocarbons and Astrophysics*, ed. Léger, A., d'Hendecourt, L., Boccara, N., Dortrecht, Reidel, 387
Lambert, D. L., Gustafsson, B., Eriksson, K., Hinkle, K. H. 1986, *ApJS*, 62, 373
Lattanzio, J. C. 1986, *ApJ*, 311, 708
Lewis, R. S., Amari, S., Anders, E. 1990, *Nat*, 348, 293
Maciel, W. J. 1976, *A&A*, 48, 27
Querci, F., Querci, M., Tsuji, T. 1974, *A&A*, 31, 265
Sauval, A. J., Tatum, J. B. 1984, *ApJS*, 56, 193
Sedlmayr, E. 1993, in *Molecules in the Stellar Environment*, ed. U.G. Jørgensen, 163
Stein, S. E., Fahr, A. 1985, *J.Phys.Chem.*, 89, 3714
Tsuji, T. 1964, *Ann.Tokyo Astron.Obs.*, 2nd ser., 9
Tsuji, T. 1973, *A&A*, 23, 411
Westerlund, B. E., Azzopardi, M., Breysacher, J., Rebeirot, E. 1991, *A&A*, 91, 425
Richter, H. B. 1986, in *Evolution of Peculiar Red Giant Stars, IAU Col.*, ed. Johnson, H. R., Zuckermann, B., Cambridge, 106, 35
Willson, L. A., Bowen, G. H. 1986 in *Lecture Note in Physics*, 254, ed. Zeilik M., Gibson D. M., Berlin, Springer, 385

This article was processed by the author using Springer-Verlag LaTeX A&A style file *L-AA* version 3.